Model-based characterization of permanent magnets with a 3D Hall-Sensor array

Daniel Cichon, Rafael Psiuk

Fraunhofer Institute for Integrated Circuits IIS
91058 Erlangen, Germany
e-mail: daniel.cichon@iis.fraunhofer.de

Abstract—Demagnetization and defects of permanent magnets used in electric drives can occur during their production or due to operating stresses and lead to reduced reliability and performance. In this paper a novel technique for magnet quality monitoring is proposed. It uses an array of 3D Hall-Sensors to measure the magnetic flux density in the proximity of the magnet. The measurement system and the expected defects are modeled analytically. Based on this model an optimal estimation method for nonlinear systems is used to determine the critical parameters of the magnet. For these parameters pass/fail limits can be applied for production tests and quality monitoring. During our research simulations and measurements were carried out to validate the proposed method.

Keywords—permanent magnets; error diagnosis; nonlinear state estimation; magnetic field camera; magnet inspection; 3D Hall sensor

I. INTRODUCTION

Rare earth magnets underlie errors due to their production process and stresses during operation. The deviation from the ideal magnetization can occur uniformly over the magnets volume or locally at spots in the magnet. Depending on the magnetization procedure it may occur that the magnet is not completely magnetized which results in a magnetization offset with respect to the nominal value and direction. Mass produced permanent magnets may also suffer from shape variations in width and thickness [1]. Both categories of errors reduce or deform the magnetic flux density.

This can cause problems when the magnet is used in a position measurement system or in an electric drive. Reduced performance or cogging torques appears [2]. To minimize these effects a variety of motor design techniques are proposed [3][4]. Other techniques based on current, voltage or vibration data were developed to monitor the motor state [5][6]. These methods use indirect quality parameters to evaluate the motors condition. In [5] a method for magnet characterization is developed which uses a Hall probe to analyze the magnetic field in the motor. In [7] results from a measurement system are presented that uses an array of 1D Hall-sensors together with an optimization technique for inline magnet inspection.

This paper proposes a methodology to examine the magnets quality after production or during operation and thus avoid performance issues related to magnet imperfections. The proposed monitoring is based directly on the magnetic flux density measured by an array of 3D Hall sensors.

II. METHODOLOGY

To evaluate the magnet's quality the field of the magnet is measured by an array of CMOS Hall-sensors. The resulting vector field of flux densities is compared to a parametrized analytical model of the magnet. The fault detection consists of two different mechanisms. In the first stage deviations of single parameters from the model are detected and quantified using an estimation algorithm. In the second stage unpredictable errors sum up to a scalar quality indicator.

The parameters that are in the focus of the paper are the magnet's geometry and the magnetization direction. Due to the nonlinearity of the magnetic field model the estimation is performed by an algorithm for nonlinear problems. The Unscented Kalman Filter meets the requirements of the application and has low computational effort [8]. The method can be performed in real time and allows a fast and accurate characterization of magnets.
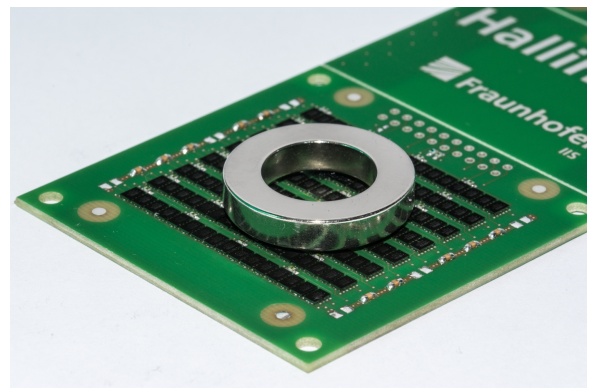

Fig. 1. Magnetic field camera developed at the Fraunhofer IIS

978-1-5090-2909-9/16/$31.00 ©2016 European Union

III. Measurement System

For the measurement of the magnetic flux density we use an array of 256 3D Hall-sensor elements. This so-called magnetic field camera (see Fig. 1) consists of integrated mixed signal circuits in chip scale packages. The sensors are based on a standard CMOS process and use the HallinOne®.technology which makes the integration of 3D Hall-sensors without nonlinear materials like concentrators possible. This allows for a high dynamic range (100µT-1T) and linearity. Each of the sensors measures the complete 3D vector $(B_x, B_y, B_z)^T$ at a distinct position. The sensor elements are arranged in a plane with a pitch of 2.5mm. On the surface of the magnetic field camera a permanent magnet can be placed. The position of the magnet can be fixed by a mechanical stop. The camera's complete measurement vector y consists of 256*3 values and can be sampled with a frequency of 100Hz. For testing purposes at real time a subset of the sensor elements can be chosen by a graphical user interface. This way experiments with different sensor configurations can be performed to determine the optimum number and position of the sensors.

IV. Measurement Model

The parameter estimation algorithm is based on a model of the magnet. In this paper a bar magnet will be examined as an example. Many other magnet shapes like cylinders or spherical magnets and their logical combinations can be modeled accordingly. This leads to an analytic or quasi-analytic solution for the model. Instead of an analytical approach the model could also be derived from a Finite Element Method. However an analytical model is much easier parametrizable and allows a better understanding of the underlying physical principles. Furthermore it allows a fast calculation of the measurement model. In the following the basics of derivation of the mathematical model are outlined.

A. Ideal permanent magnet model

One can derive the analytical expression for the magnetic field components of a rectangular bar magnet using the Poisson equation for the scalar magnetostatic potential [9]. The magnetic flux density in air can be calculated with:

$$B(r) = -\mu_0 \nabla_r \Phi(r) \tag{1}$$

With $r=(x,y,z)^T$.

The solution of the scalar potential for a magnet with a magnetization M_x along the x-axis can be obtained using Gauss` law:

$$\Phi(r) = -\frac{M_x}{4\pi}\frac{\partial}{\partial x} \int_{-\frac{xb}{2}}^{\frac{xb}{2}} \int_{-\frac{yb}{2}}^{\frac{yb}{2}} \int_{-\frac{zb}{2}}^{\frac{zb}{2}} \frac{dx_i dy_i dz_i}{\sqrt{(x-x_i)^2+(y-y_i)^2+(z-z_i)^2}} \tag{2}$$

Integration of eq. 2 leads to an analytic expression for the scalar magnetostatic potential.

Eq. 2 delivers the magnetic field in the magnets coordinate system. To transform the field to the cameras coordinate system we use a combination of shift and rotation transformations we apply to the vector field.
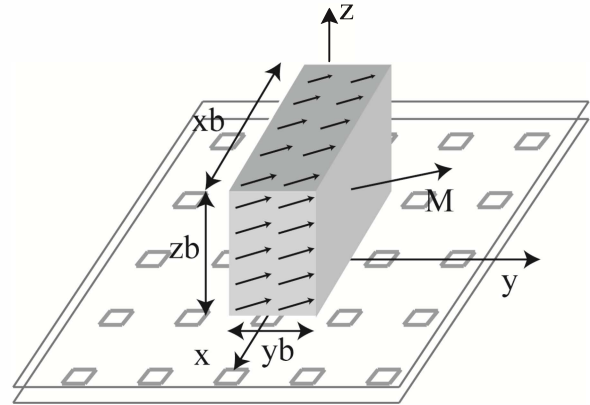

Fig. 2. Schematic illustration of the arrangement

B. Fault model

The dimensions of the magnet are critical factors for cogging torque [1]. They vary because of the manufacturing process. Another parameter which influences the magnets field is the offset of magnetization [10]. Both a deviation from its nominal remanence and a shift of the magnetization direction can occur. Measurements show, that a magnetization skew of mass produced industrial magnets lies between ±1° for high quality magnets.

Magnet geometry parameters and its magnetization are adapted directly by variation of the ideal model (see eq. 2). To model an arbitrary magnetization the model for a uniform, axis-parallel magnetization is extended. The modified model uses three elementary magnets with orthogonal magnetization. The resulting flux density is calculated by superposition of the separate bar magnets:

$$B_{total} = B_{Mx} + B_{My} + B_{Mz} \tag{3}$$

Inside the magnet the field is still homogeneous and unidirectional as shown in Fig. 2.

V. Parameter estimation Algorithm

To goal of the parameter estimation algorithm is to find the model parameters $x=(xb,yb,zb,M_x,M_y,M_z)^T$ which fit the measured values y. A classical approach is to minimize

$$\Delta = ||y - h(x)|| \tag{4}$$

With a Bayesian framework it is possible to solve the inverse problem of eq. 4 and incorporate a priori information on the system. The Kalman Filter is an algorithm which uses

this approach. It calculates recursively the mean for every element of x and the corresponding covariance matrix P. To describe the system a time-update f(x) and a measurement function h(x) are used. The function h(x) is calculated from eq. 1-3. In the case of a system with only nondeterministic parameter variations the uncertainty about the state can be modeled by a Gaussian process with the covariance matrix Q and the time update function f(x)=x. The unscented transform is used to make the Kalman Filter applicable to nonlinear systems. The so-called sigma points $\tilde{x}$ represent the probability distributions and propagate mean and covariance through the time and measurement update functions. The main steps of the algorithm are described in the following.

The algorithm is initialized with the following a priori state $\hat{x}_0{}^+$ and covariance $P_0{}^+$:

$$\hat{x}_0^+ = (xb_0, yb_0, zb_0, M_{x0}, M_{y0}, M_{z0})^T \tag{5}$$

$$P_0^+ = E[(x_0 - \hat{x}_0^+)(x_0 - \hat{x}_0^+)^T] \tag{6}$$

Here M_x, M_y, M_z denote the magnetization of the magnet in the direction x, y and z. P is initialized with the covariance of the initial guess. The nominal values and tolerances from the manufacturer are used as a starting point. After this initialization the following calculations are repeated recursively. Due to the linearization error caused by the unscented transform, several iterations are performed until a steady state is reached.

In the next step the sigma points are calculated around the previous/initial state:

$$\hat{x}_{k-1}^{(i)} = \hat{x}_{k-1}^+ + \tilde{x}^{(i)} \quad i = 1, \dots, 2n \tag{7}$$

$$\tilde{x}^{(i)} = \left(\sqrt{nP_{k-1}^+}\right)_i^T \quad i = 1, \dots, n \tag{8}$$

$$\tilde{x}^{(n+i)} = -\left(\sqrt{nP_{k-1}^+}\right)_i^T \quad i = 1, \dots, n \tag{9}$$

Here n denotes the number of degrees of freedom. In our case n=6.

The sigma points are propagated through the dynamic model and the predicted measurement values ŷk(i) are calculated. The corresponding covariances P, Py and Pxy are calculated.

$$\hat{x}_k^{(i)} = f\left(\hat{x}_{k-1}^{(i)}\right) = \hat{x}_{k-1}^{(i)} \tag{10}$$

$$\hat{x}_k^- = \frac{1}{2n} \sum_{i=1}^{2n} \hat{x}_k^{(i)} \tag{11}$$

$$P_k^- = \frac{1}{2n} \sum_{i=1}^{2n} \left(\hat{x}_k^{(i)} - \hat{x}_k^-\right)\left(\hat{x}_k^{(i)} - \hat{x}_k^-\right)^T + Q \tag{12}$$

$$\hat{y}_k^{(i)} = h\left(\hat{x}_k^{(i)}\right) \tag{13}$$

$$\hat{y}_k = \frac{1}{2n} \sum_{i=1}^{2n} \hat{y}_k^{(i)} \tag{11}$$

$$P_y^- = \frac{1}{2n} \sum_{i=1}^{2n} \left(\hat{y}_k^{(i)} - \hat{y}_k\right)\left(\hat{y}_k^{(i)} - \hat{y}_k\right)^T + R \tag{15}$$

$$P_{xy}^- = \frac{1}{2n} \sum_{i=1}^{2n} \left(\hat{x}_k^{(i)} - \hat{x}_k^-\right)\left(\hat{y}_k^{(i)} - \hat{y}_k\right)^T \tag{16}$$

Q is the process noise covariance and R is the noise of the Hall-Sensors. Both quantities are constant diagonal matrices.

In the last step the so-called Kalman-Gain K is calculated and x and P are updated.

$$K_k = P_{xy}P_y^- \tag{17}$$

$$\hat{x}_k^+ = \hat{x}_k^- + K_k(y_k - \hat{y}_k) \tag{18}$$

$$P_k^+ = P_k^- - K_k P_y K_k^T \tag{19}$$

Here y_k is the measurement vector of the magnetic field camera. The term $(y_k - \hat{y}_k)$ in (15) is called innovation. It is the part of the measurement that contains new information and updates the state estimate [8]. For a linear Kalman Filter with the linear measurement matrix H it can be shown, that the innovation term has zero mean and a white power spectral density. In this case the covariance equals:

$$E\left[(y_k - \hat{y}_k)(y_k - \hat{y}_k)^T\right] = H_k P_k^- H_k^T + R_k \tag{20}$$

If the innovation's noise spectrum is colored or if its mean is not zero or if it has the wrong covariance the model does not fit the measurements. In this case the magnet produces a vector field that cannot be described by the measurement model. Thus these quantities can serve as indicators for the quality of the magnet. We use the offset of the innovation to calculate a figure of merit (FOM). It is calculated as the difference between the maximum and minimum of the innovation vector elements:

$$FOM = |Max[y - \hat{y}_k] - Min[y - \hat{y}_k]| \tag{21}$$

VI. SIMULATIONS

To verify the proposed method we performed simulations with the following boundary conditions. A magnet and sensors with the parameters listed in TABLE I. was assumed. We generate sinusoidal signals with different frequencies for every parameter. This way the magnetization vector is rotated and the magnet size is modulated during the simulation simultaneously in a systematic way. To take measurement

errors into account we add white noise to the simulated measurements. Fig. 3 and Fig. 4 show the results of the simulation. The graphs show the absolute error x_{actual}-$x_{estimated}$ of the magnet geometry and the magnetization. The solid lines are the result of a single simulation. The dashed lines show the average absolute deviation gained from a set of 100 Monte-Carlo-Simulations with random sensor noise.

The simulation shows that the magnet size can be estimated with an accuracy of 3μm. The remaining error depends on the

TABLE I. SIMULATION PARAMETERS

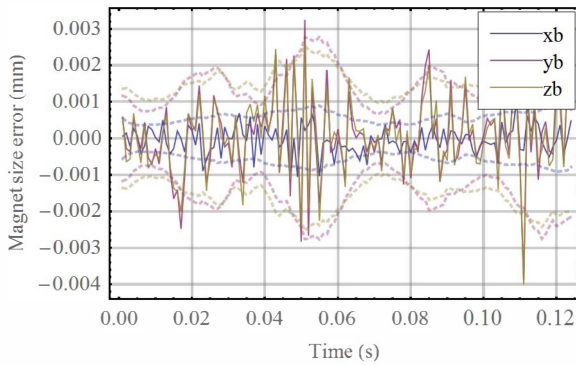| Parameter	Description	Nominal value	Stimulation range
xb	Length	19.1 mm	+-1mm
yb	Width	12.7 mm	+-1mm
zb	Height	6.4 mm	+-1mm
M_x	Magnetization x	0	+-100A/m
M_y	Magnetization y	980 kA/m	+-100A/m
M_z	Magnetization z	0	+-100A/m
R	Sensor noise standard deviation	10μT	

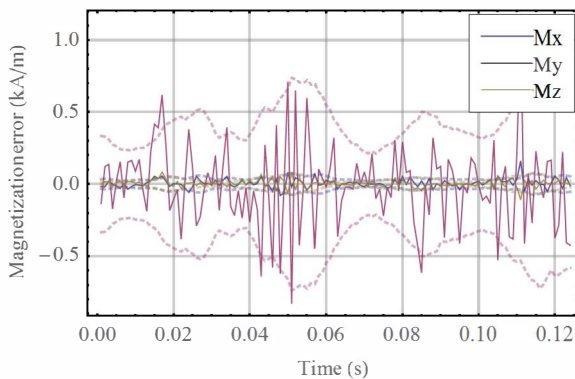Fig. 3. Estimation error for the magnet size

Fig. 4. Estimation error for the magnetization

axis. The parameter xb can be measured more accurately than zb. The error increases with zb, if the center of the magnet moves away from the sensor array. The error bounds for the magnetization lie between +-0.7kA/m. This corresponds to a magnetization offset angle of 0.04°.

VII. MEASUREMENTS

For a practical evaluation of the method we characterized 40 bar-shaped permanent magnets as defined in TABLE I. In a second test magnets with mechanical defects were investigated. All the measurements were performed at room temperature (25°C). The described algorithm was used to estimate the magnet parameters. To reach a steady state and minimize the linearization errors, 100 measurement and estimation cycles were performed before the values were stored. Experiments with different sensor arrangements showed that an array of 5x6 3D Hall-sensors with a pitch of 5mm delivers enough information about the magnetic field distribution. The use of more elements from the magnetic field camera does not increase the accuracy of the estimation significantly.

For a first verification of the method 20 magnets were positioned successively on the magnetic field camera and then rotated 180° about their y-axis. The magnetization M was estimated before (M) and after the rotation (M'). With the assumed model the resulting magnetization directions should rotate with the magnet ($M_x=M_x'$ and $M_z=-M_z'$). Fig. 5 shows the results for both placements of each magnet.
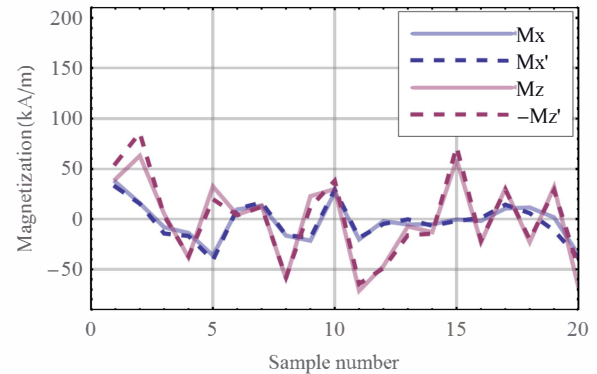

Fig. 5. Magnetization Mx and Mz for different orientations on camera

The measured results are consistent with the theory. The standard deviation of the measurement uncertainty is below 6kA/m.

Fig. 6 and Fig. 7 show the measured distribution of the magnetization direction. The dashed line shows the fitted distribution assuming a Gaussian process. The standard deviation for the characterized magnet is 19kA/m for M_x and 41kA/m for M_z respectively. This corresponds to a magnetization angle offset of 1.1° and 2.3°. The main magnetization M_y has a standard deviation of 28kA/m.

The results for the estimation of the magnet size xb are shown in Fig. 8. The estimated value is smaller than the magnets actual mechanical length (19.1mm). This effect can be partially explained by the magnets' protective coating. The standard deviation of 55μm is consistent with the manufacturer's specified tolerance.
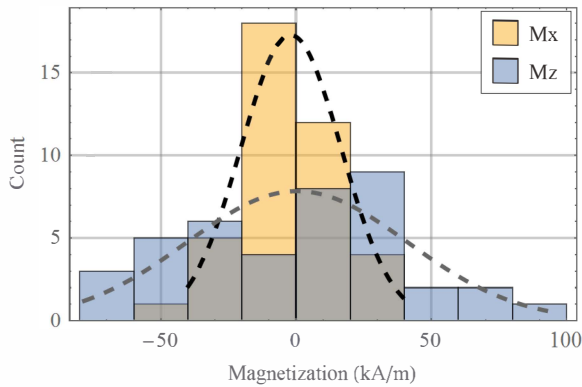
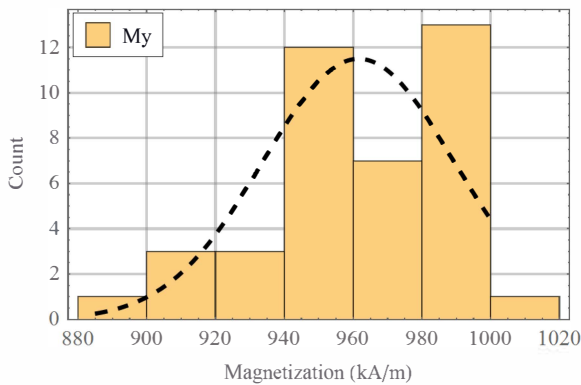Fig. 4. Magnetization Mx and Mz for different magnets
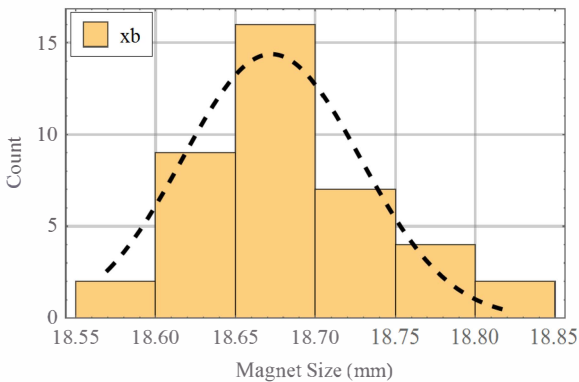

Fig. 5. Magnetization My for different magnets

Fig. 6. Magnet size *xb* for different magnets

In the second test scenario magnets with defects were investigated using the method and FOM as previously described. We damaged the magnets in two different ways. For the first test we grinded off 4mm of the magnet's edge to emulate a mechanical error. In the second test we heated the magnets up to a defined temperature to investigate a magnetization change close to the Curie temperature (310°C). Thereby we first exposed one side of the magnet to high temperature while the other side was connected to a heat sink. Afterwards the magnet was heated uniformly. TABLE II. shows the results for the estimation of the relevant parameters.

TABLE II. CHARACTERIZATION OF DAMAGED MAGNETS

Description	Size (mm)	Magnetization (kA/m)	FOM (mT)
Undamaged magnet[a]	18.7; 5.51; 12.3	-5.6/952/-4.1	0.99
Grinded magnet	16.9/5.67/14.0	2.0/959/8.6	3.56
Partially heatet (T=200°C)	18.9/5.08/11.9	2.3/726/0.18	5.18
Partially heatet (T=300°C)	18.5/2.97/9.16	-11/1300/-1.9	8.29
Uniformly heated (T=300°C)	19.9/5.50/13.6	2.0/303/0.13	0.58

[a.] Mean values from all investigated magnets.

The characterization of the grinded magnet led to a significantly higher FOM value, the other parameters also indicated a deformation. Partial heating of mechanically undamaged magnets changed the estimated magnetization and FOM as expected. A deformation of the estimated magnet geometry could be observed at 300°C. This magnetic deformation was reversed when the magnet was heated uniformly. The degradation of the estimated magnetization value remained so the magnet's damage could still be measured.

VIII. SUMMARY

A method for testing permanent magnets using an array of 3D Hall-sensors has been proposed in this paper. An analytical model including expected magnetic deformations was derived for a simple magnet shape. Measurements of a magnetic field camera were used as input for a parameter estimation algorithm. The method was verified by simulations and the limits for the accuracy were evaluated. It has been shown that an offset of magnetization and the dimensions of the magnet can be estimated using the described algorithms and arrangement. Measurement results from a sample quantity of mass-produced magnets with different imperfections were presented. They show that common errors can be detected and quantified. The method can be used to assure permanent magnets' quality in production or maintenance of electric drives and thus improve performance and reliability at a low effort.

REFERENCES

[1] L. Gasparin, A. Cernigoj, S. Markic and R. Fiser, "Additional Cogging Torque Components in Permanent-Magnet Motors Due to Manufacturing Imperfections," in IEEE Transactions on Magnetics, vol. 45, no. 3, pp. 1210-1213, March 2009.

[2] J. Asama, K. Samejima, T. Oiwa and A. Chiba, "Investigation of permanent magnet magnetization for a bearingless servomotor," 2013 IEEE Energy Conversion Congress and Exposition, Denver, CO, 2013, pp. 4306-4311.

[3] N. Bianchi and S. Bolognani, "Design techniques for reducing the cogging torque in surface-mounted PM motors," in IEEE Transactions on Industry Applications, vol. 38, no. 5, pp. 1259-1265, Sep/Oct 2002.

[4] M. Klausnitzer and A. Möckel, "Quick cogging torque calculation for electronically commutated motors considering combinations of deviant and flawless magnets," Power Electronics, Electrical Drives, Automation and Motion (SPEEDAM), 2012 International Symposium on, Sorrento, 2012, pp. 66-69.

[5] M. Brela, M. Michalski, H. J. Gebhardt and J. Franke, "Hall measurement method for the detection of material defects in plastic-embedded permanent magnets of rotors," Industrial Electronics Society,

IECON 2013 - 39th Annual Conference of the IEEE, Vienna, 2013, pp. 3928-3934.

[6] J. A. Farooq, A. Djerdir and A. Miraoui, "Analytical Modeling Approach to Detect Magnet Defects in Permanent-Magnet Brushless Motors," in IEEE Transactions on Magnetics, vol. 44, no. 12, pp. 4599-4604, Dec. 2008.

[7] K. Vervaeke, "Inline magnet inspection using fast high resolution MagCam magnetic field mapping and analysis", Electric Drives Production Conference (EDPC), 2011, pp. 172-180

[8] Simon, D., Optimal state estimation: Kalman, H infinity, and nonlinear approaches, John Wiley & Sons, 2006.

[9] Engel-Herbert, R.; Hesjedal, T., "Calculation of the magnetic stray field of a uniaxial magnetic domain", Jornal of Applied Physics, vol. 97, 2005.

[10] H. Qian, H. Guo, Z. Wu and X. Ding, "Analytical Solution for Cogging Torque in Surface-Mounted Permanent-Magnet Motors With Magnet Imperfections and Rotor Eccentricity," in IEEE Transactions on Magnetics, vol. 50, no. 8, pp. 1-15, Aug. 2014.